Supporting Information

Microencapsulated Linseed Oil Adhesive Based on Photosensitive Indication: A Smart Material for Visualized Curing Monitoring

Jingjing Ren[1], Shouzheng Jiao[1], Zhengyu Chen[2], Li An[1], Ran Mo[1], Fanghua Pan[1], Yuwei Hao[1], Taolin Zhang[1], Lu Han[1], Ruping Liu[1], Zhicheng Sun[1]*, Zhongjun Cheng[3]**

[1]Beijing Engineering Research Center of Printed Electronics, School of Printing and Packaging Engineering, Beijing Institute of Graphic Communication, Beijing 102600, P. R. China

[2]Yangzhou Xianghua New Material Technology Co. Ltd., Jiangsu 225000, PR China

[3]State Key Laboratory of Urban Water Resource & Environment, School of Chemistry and Chemical Engineering, Harbin Institute of Technology, Harbin 150001, P. R. China

E-mail: sz.jiao@outlook.com; sunzhicheng@bigc.edu.cn; chengzhongjun@iccas.ac.cn

1.Materials

All chemicals and solvents were purchased from commercial sources and used as received without further purification. Sodium alginate (SA), calcium chloride ($CaCl_2$), tween 80 were purchased from Inokai Technology Co., Ltd. Sundried linseed oil was acquired from Zhejiang Rubens Technology Co., Ltd. The 1-(2-Hydroxyethyl)-3，3-dimethylindolino-6/'-nitrobenzopyrylospiran was purchased from Shanghai Linen Technology Development Co., Ltd.

2.Characterization instruments and methods

The microstructure, particle characteristics of the microcapsules were characterized using environmental scanning electron microscopy (TESCAN MIRA LMS, Czechia). The microcapsule samples were placed in a carrier channel within a low voltage vacuum environment, and clear morphological images were obtained at an acceleration voltage of 20.0 KV. The chemical structure of the microcapsules was analyzed using a Fourier transform infrared spectrometer (Thermo Fisher Scientific Nicolet iS20, USA). The FTIR spectrometer recorded spectra with a resolution of 4 cm^{-1} in the wavelength range of 400 cm^{-1} to 4000 cm^{-1}. The particle size and distribution of the microcapsules were analyzed using a Malvern laser particle size analyzer (Malvern Mastersizer 3000+ Ultra, UK).The rheological behavior, specifically the viscosity modulus, of the microcapsules was investigated using a rotational rheometer (HAAKE MARS40, Thermo Fisher Scientific, USA) with a heating rate of 5 $^{o}C•min^{-1}$.The lap-shear test was performed on a universal testing machine (CMT6103 MTS, USA) at a speed of 50

mm•min^{-1}. Thermogravimetry Analysis (TG) (TA Q500, USA) was carried out in an Nitrogen atmsphere at 50 mL•min^{-1} with a temperature increase rate of 10 °C•min^{-1}, and the measurement temperature interval was 30-800 °C. Differential scanning calorimetry (DSC) (Netzsch DSC214, Germany) was performed in the temperature range of 30-160 °C with a ramp rate of 10 °C•min^{-1}.

To evaluate the formation of oxidative byproducts during the curing process of microencapsulated linseed oil adhesive (MLOA), a 2-thiobarbituric acid (TBA) colorimetric assay was conducted to quantify the extent of lipid peroxidation. TBA is known to react specifically with malondialdehyde (MDA), a representative secondary oxidation product of unsaturated fatty acid chains, to form a stable chromogenic complex with a characteristic absorbance at 530 nm, enabling sensitive detection of oxidative degradation. The TBA reagent was prepared by dissolving 200 mg of 2-thiobarbituric acid in 100 mL of n-butanol and allowing the solution to stand at room temperature for 15 h, followed by filtration. MLOA samples were first thermally cured at controlled temperatures (20 °C, 40 °C, 60 °C, 80 °C, and 100 °C) for 2 h under ambient air. After curing, each sample was accurately weighed and dissolved in n-butanol, followed by dilution to a final volume of 25 mL. A 5 mL aliquot of this solution was then mixed with 5 mL of freshly prepared TBA reagent and heated in a 95°C water bath for 2 h. The reaction mixture was rapidly cooled to 26 ± 2 °C, and the absorbance (A_a) was measured at 530 nm using a UV-Vis spectrophotometer (PE lambda 750). A blank reference (A_b) was prepared using the same protocol with pure n-butanol instead

of the MLOA sample solution. The absorbance values reflect the concentration of TBA-MDA adducts formed during curing and thus indirectly indicate the degree of oxidative polymerization. Higher absorbance corresponds to greater MDA release and a more pronounced oxidative reaction. This method allows the systematic comparison of oxidative curing efficiency across temperature conditions and offers insights into the reaction kinetics of linseed oil under confined core-shell microenvironments.

$$TBARS = \frac{50 \times (A_a - A_b)}{m} \#(1)$$

where *m* is the weight of the sample (mg).

The curing conversion (α) of the linseed oil phase was quantified by FTIR spectroscopy based on the progressive consumption of C=C functional groups during curing. Infrared spectra collected over the curing period (0-10 h) were analyzed using absorbance as the vertical axis. After baseline correction, the integrated area of the characteristic C=C absorption band was determined at each curing time, with the spectrum at 0 h taken as the reference corresponding to the uncured state with the highest concentration of C=C bonds. The curing conversion at a given time was calculated according to:

$$\alpha = \frac{A_0 - A_t}{A_0} \#(2)$$

where A_0 and A_t denote the integrated areas of the C=C absorption band at 0 h and time, respectively. The decrease in the C=C peak area reflects the oxidative crosslinking of linseed oil, and thus αrepresents the fraction of double bonds that have participated in the curing reaction over time.

3.Experimental details

Microencapsulated linseed oil adhesive (MLOA) was synthesized using the Electrostatic spray method, the process and principle of which were exhibited in Figure S1. A 1 wt% sodium alginate aqueous solution was first prepared and stirred thoroughly using a magnetic stirrer. Linseed oil was then added at a fixed mass ratio of 5:1 (sodium alginate solution to linseed oil), followed by the addition of a suitable amount of Tween 80, 1 wt% cobaltous naphthenate, and 1 wt% spiropyran. The resulting mixture was emulsified under an ice bath to maintain materials stability during emulsification. The obtained emulsion was loaded into a 10 mL syringe, which was connected to a high-voltage power supply. Under controlled electrospraying conditions, the emulsion was gradually ejected through the needle and directly introduced into a 1 wt% calcium chloride aqueous solution. Upon contact, the sodium alginate in the emulsion immediately reacted with calcium ions, forming an ionically cross-linked calcium alginate network that served as the shell material. Concurrently, linseed oil remained encapsulated within the core, thereby forming MLOA.

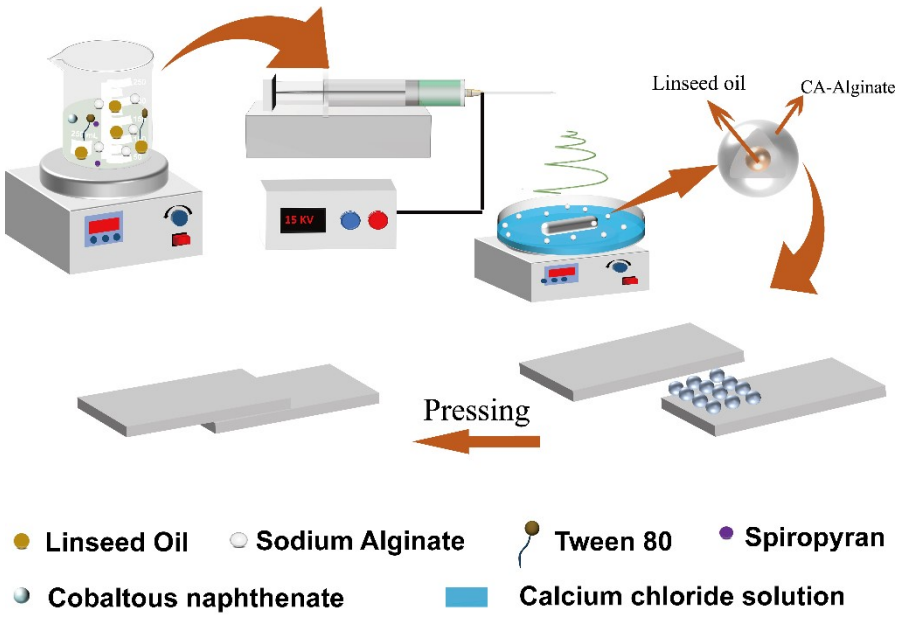

Figure S1. Schematic illustration of the mechanism of preparing Microencapsulated linseed oil adhesive by Electrostatic spray method.

Electrospraying is a commonly used physical method for the preparation of microcapsules, characterized by its simple operation and high efficiency. In this study, the prepared adhesive system is predominantly bio-based, with linseed oil as the main renewable component. Based on the formulation ratio of the core and shell materials, the overall bio-based content was calculated to be approximately 92-94 wt%. During the process, when the emulsion droplets are sprayed into a calcium chloride solution, rapid ionic crosslinking occurs, resulting in the immediate formation of a solid shell structure. Similar to common drying oils like linseed oil, they are rarely used in research due to their slow drying and curing rates, so metal salts (i.e., drying agents) are often added to them. Therefore, in this study, a cobalt drying agent was introduced to accelerate all reactions involved in oxidation and surface solid film formation, thereby promoting the curing reaction. [1] In addition, to prevent premature oxidation of linseed

oil, the emulsification process was carried out in a sealed vessel under ice-bath conditions, and during electrospraying, a high voltage and flow rate were employed to ensure rapid encapsulation upon contact with the $CaCl_2$ solution. This effectively minimized oxygen exposure and maintained the core material in an unreacted state before capsule rupture.

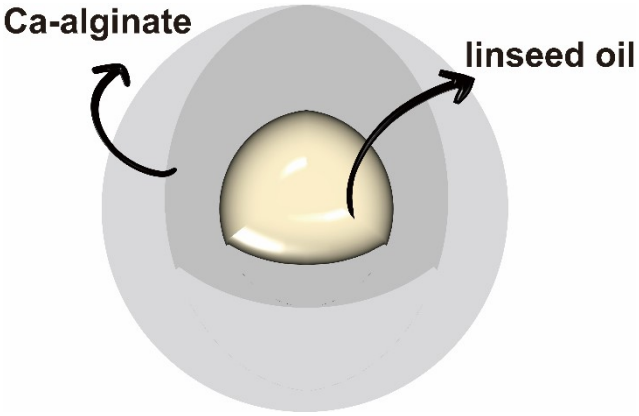

Figure S2. Schematic diagram of the structure of MLOA.

The prepared MLOA exhibits a shell-core structure, in which the core material is linseed oil, meanwhile, spiropyran was added in the core as the indicator and the shell material is calcium alginate.

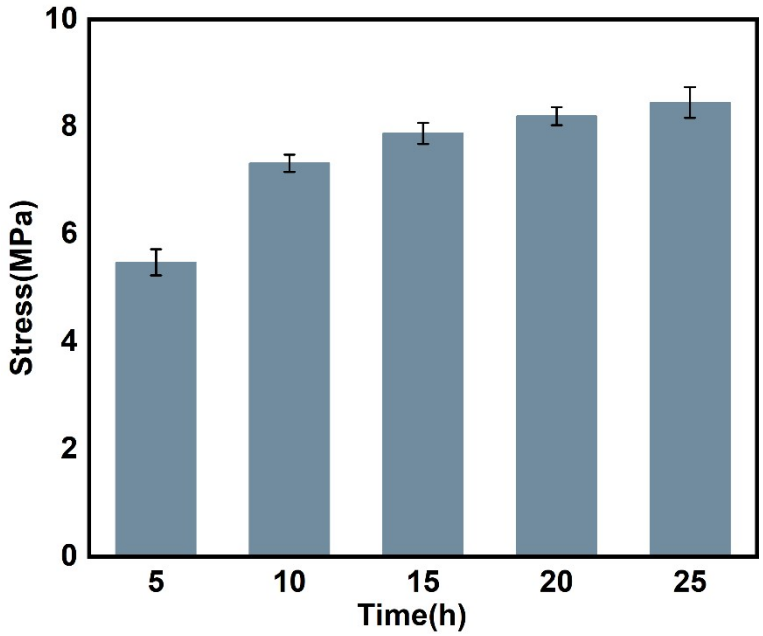

Figure S3. Relationship between Curing Time and Adhesive Strength of MLOA

The adhesive strength of the MLOA increased significantly during the initial curing stage (5-10 h) and then rose more slowly from 15 h to 25 h. The apparent reduction in the growth rate after 10 h indicates that the oxidative crosslinking reaction gradually approaches completion, suggesting that the adhesive system can be regarded as essentially fully cured after approximately 10 h, with only marginal strengthening upon further curing to 15-25 h. Notably, this curing stage coincides with the stabilization of the color change, confirming that the visual color evolution provides a reliable and intuitive indicator of the curing degree and can be used to assess curing completion without additional instrumentation.

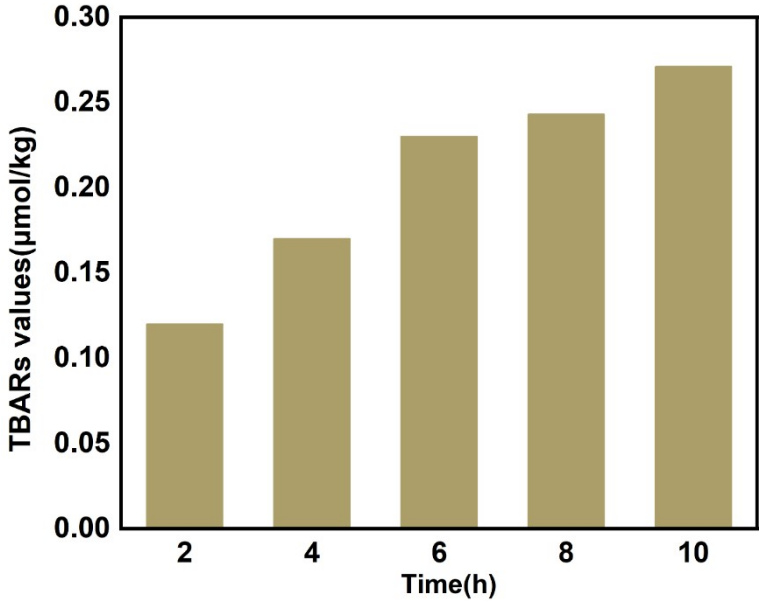

Figure S4. Relationship between curing time and TBARS values

The TBARS values of the MLOA samples increased monotonically with curing time (2-10 h), indicating the continuous accumulation of oxidative by-products during the crosslinking process. As an independent chemical assay, the TBARS analysis provides quantitative supporting evidence for the progression of oxidative curing and thus substantiates the curing conversion evaluated from FTIR measurements. In parallel, the color difference (ΔE) exhibits a systematic decrease as curing proceeds and the network structure becomes more consolidated. The consistent trends observed from TBARS analysis, FTIR-derived conversion, and ΔE evolution demonstrate that the color change is quantitatively correlated with the curing degree rather than being a merely qualitative visual effect, thereby supporting its use as a measurable indicator to assist the assessment of curing conversion.

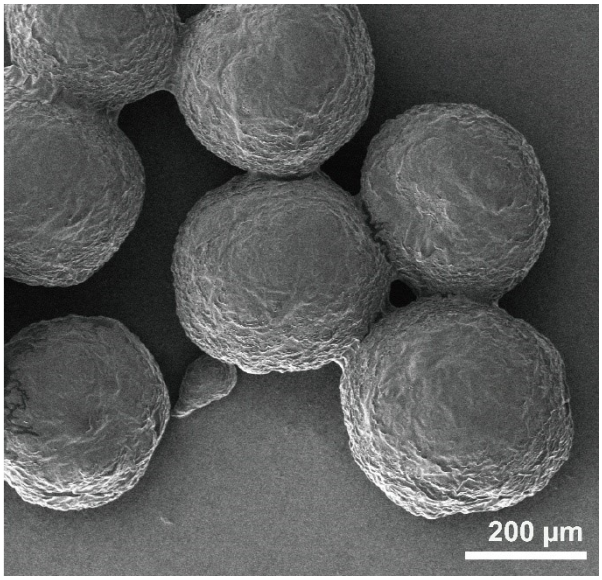

Figure S5. SEM image of MLOA.

The prepared MLOA microcapsules exhibited a well-defined spherical morphology with relatively large and uniform particle sizes. This structure allows for efficient encapsulation of a significant amount of linseed oil while maintaining good size uniformity.

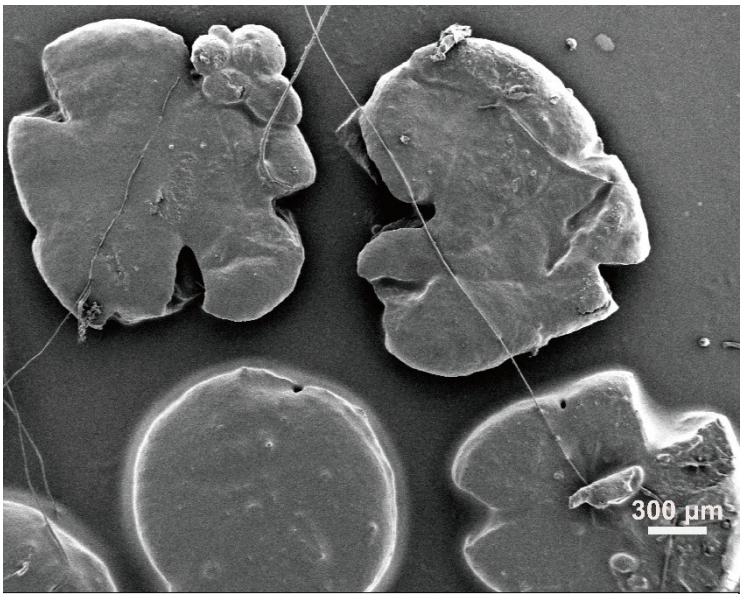

Figure S6. SEM image of MLOA after being broken by applying a certain external force.

After breakage, the MLOA presents an irregular and collapsed shape, with clear edge fractures and partial collapse of the shell structure, showing a shell-core structure.

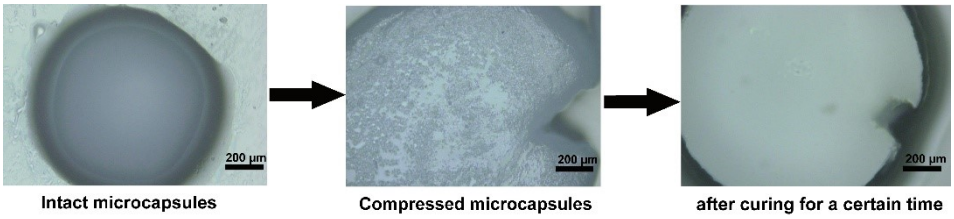

Figure S7. Schematic of the process of the fragmentation and solidification of MLOA.

Under laser confocal microscopy, three states of MLOA can be observed: in the intact state, it exhibits a distinct shell-core structure; when compressed, the MLOA shows obvious cracks, allowing the core material to rapidly contact oxygen; and after curing for a certain period, the MLOA gradually becomes transparent. When an external force is applied to the MLOA microcapsules, they rupture and release the encapsulated linseed oil. Upon exposure to air, the linseed oil comes into contact with oxygen and undergoes oxidative crosslinking, thereby initiating the adhesive process.

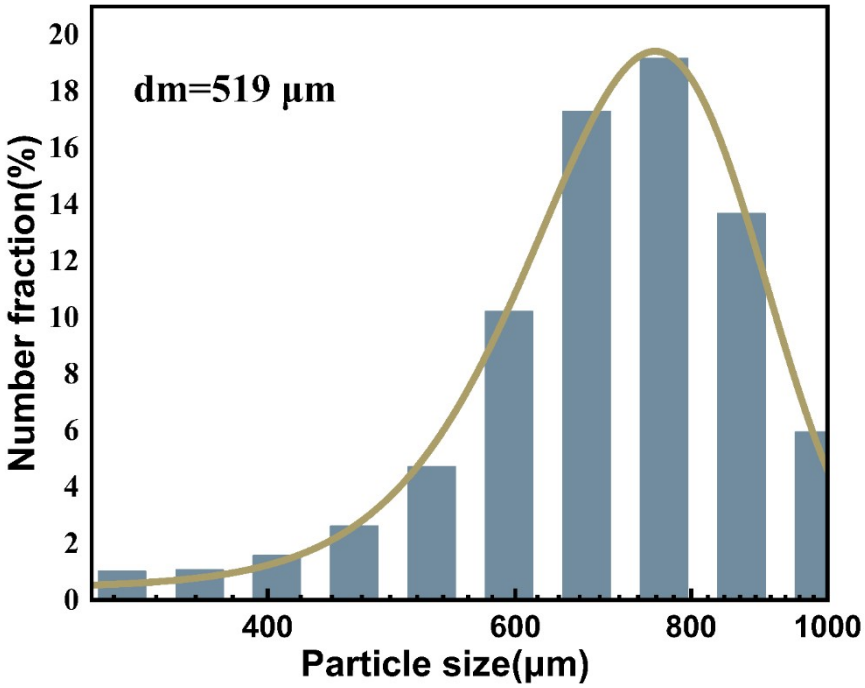

Figure S8. Particle size distribution of MLOA determined by Laser particle size analysis.

The microcapsules obtained under the described preparation conditions exhibited an average particle size of approximately 500 μm with a uniform size distribution. This size range meets the requirements for most subsequent characterization and performance tests. Therefore, unless otherwise specified, all experiments in this work were conducted using adhesive microcapsules of this size.

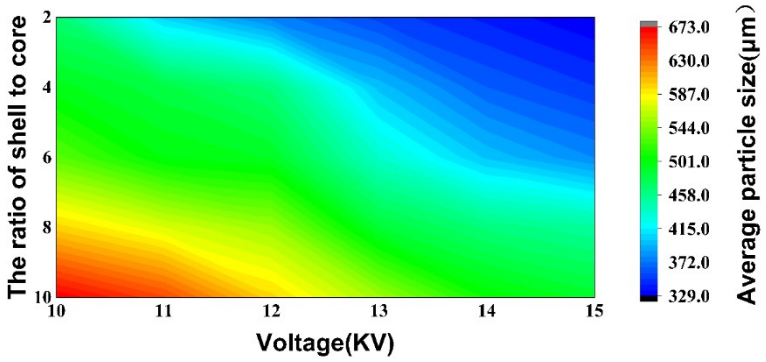

Figure S9. Average particle size of microencapsulated linseed oil adhesive at different under different voltages and core-shell ratios.

In order to study the preparation process of MLOA, different mass ratios of shell materials to core materials and different voltage values were adopted to prepare MLOA. Figure S10 shows the influence of different mass ratios of shell materials to core materials and different voltage values on the size of MLOA. When the mass ratio of shell materials to core materials is constant, the particle size of MLOA decreases as the voltage increases. This is because increasing the voltage can significantly reduce the particle size by enhancing the electric field force, increasing the charge density, and accelerating the jet breakup. In addition, when the voltage remains unchanged, the particle size increases with the increase of the mass of the shell material. This may be due to the increase in the mass of the shell material, which can lead to an increase in the viscosity of the solution, restricted charge conduction, or an enhanced tendency of droplet coalescence. Therefore, the controllable synthesis of MLOA can be achieved by adjusting the mass ratio of shell materials to core materials and the voltage value.

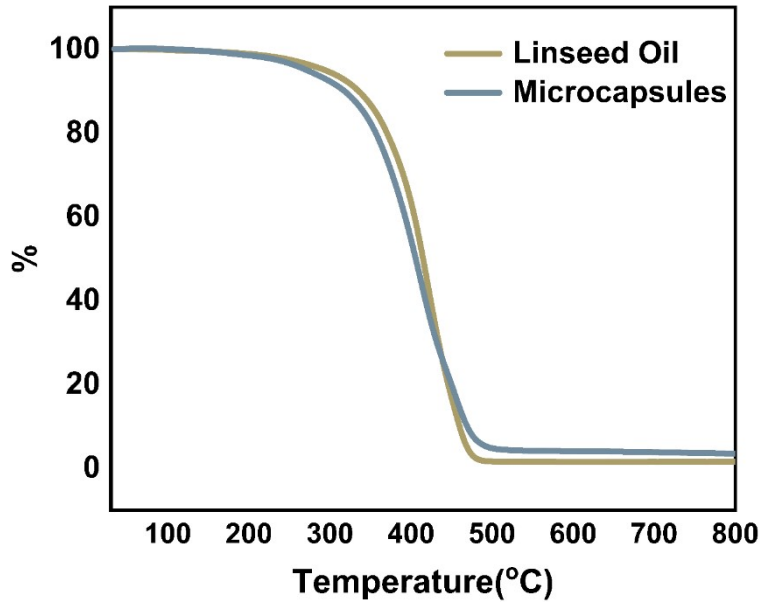

Figure S10. The thermal stability of linseed oil and Microencapsulated linseed oil adhesive.

It is obvious that the microencapsulation of linseed oil has no effect on the thermal stability of linseed oil itself, MLOA can maintain good thermal stability below 300 °C, meeting the usage requirements for daily and medium-to-high temperature environments. This meets the requirements of most adhesive application environments.

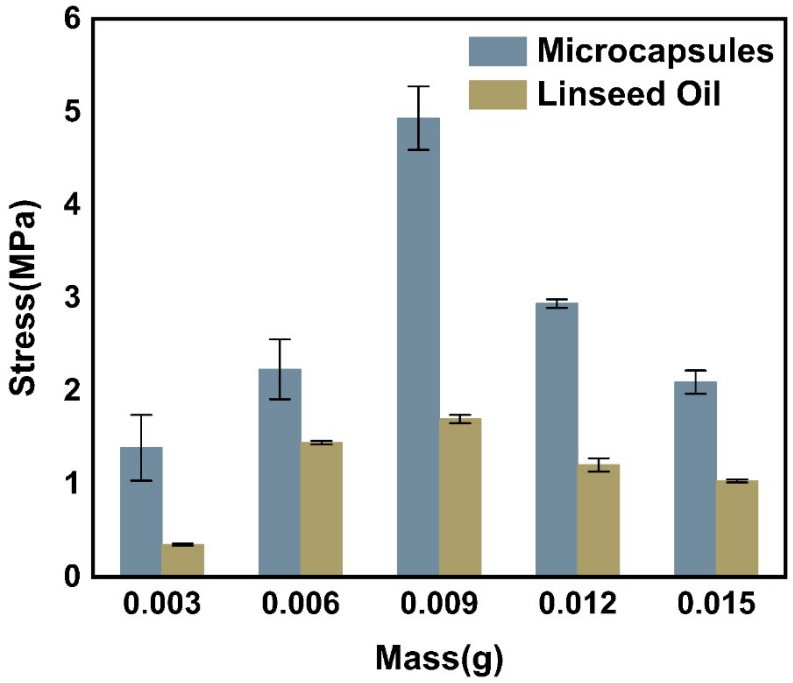

Figure S11. Comparison of the adhesion strength before and after microencapsulation of linseed oil.

The microencapsulation of linseed oil significantly enhances its adhesive performance compared to the use of bulk oil. This improvement can be attributed to two key factors. First, the encapsulation process dramatically increases the oil's effective surface area, enabling faster and more uniform exposure to atmospheric oxygen, which is essential for the oxidative curing of drying oils. Second, the incorporation of metal-based catalysts, such as cobalt salts, into the linseed oil core further accelerates the decomposition of hydroperoxides formed during oxidation. Together, these effects promote rapid crosslinking at the adhesive interface, leading to improved initial bonding strength and final mechanical stability. This dual enhancement strategy provides a valuable reference for the development of smart, self-curing adhesives based on bio-derived oils.

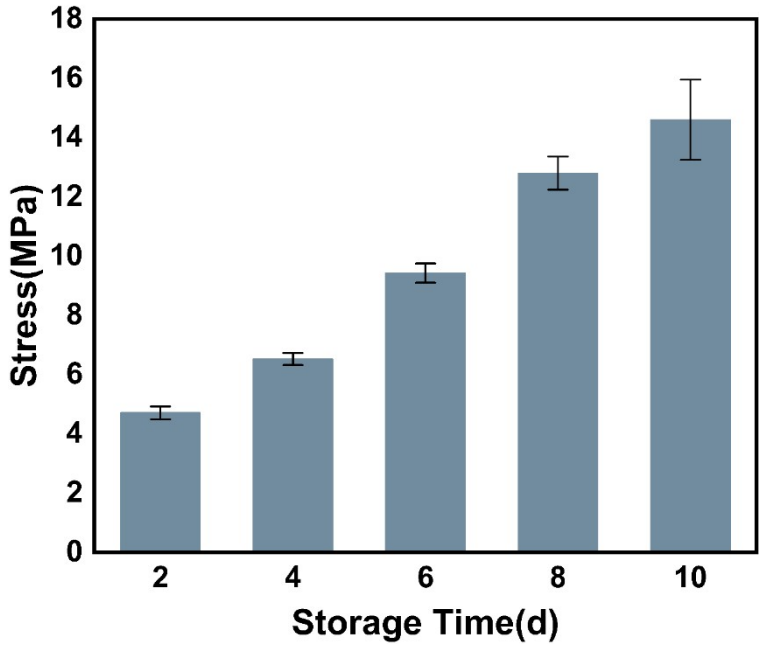

Figure S12. The adhesion strength of different storage times of MLOA with room temperature.

It is obvious that the longer the storage time, the better the adhesive performance of MLOA, because the unsaturated fatty acid chains in linseed oil will cross-link more thoroughly under a longer curing time.

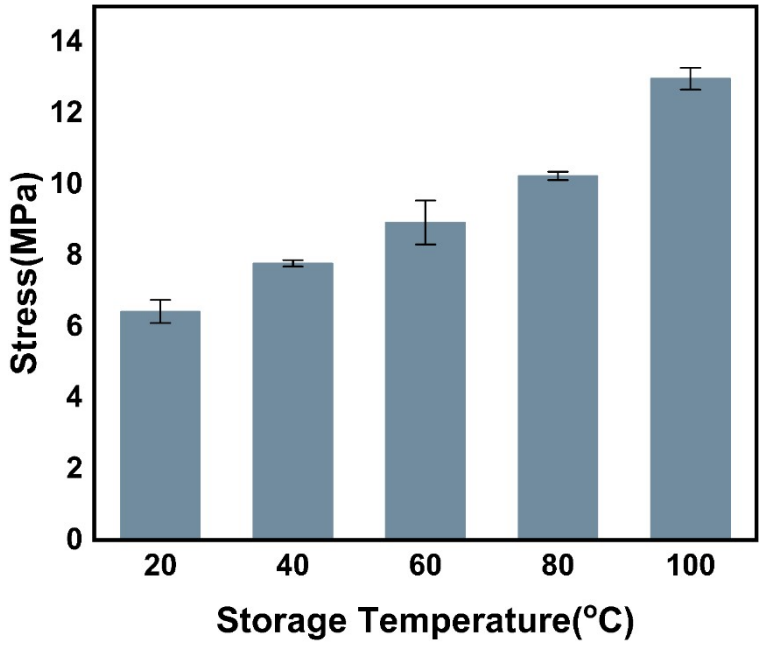

Figure S13. The adhesion strength of different storage temperature of MLOA during 24 h.

To prevent the PMMA from being damaged by high temperatures, the maximum curing temperature is set at 100 °C, which also meets the curing requirements at room temperature. When we extend the curing time at high temperatures, it also demonstrates the time-temperature synergistic effect of MLOA.

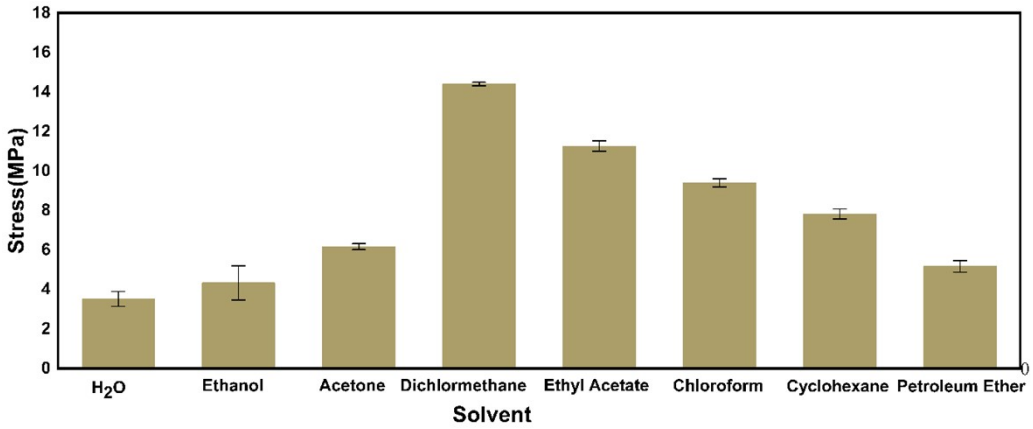

Figure S14. The adhesion strength of different solvent environment.

When MLOA is placed in solvent environments of different polarities, it is found that in highly polar solvents such as H_2O or ethanol, the lower adhesive strength stems from the fact that polar molecules react with the hydrogen bonds in the shell material, weakening the strength of the shell material and causing premature release of the core material, etc. In a low - polarity solvent environment, according to the principle of "like dissolves like", polar molecules will extract linseed oil, thus leading to a decrease in adhesive force.

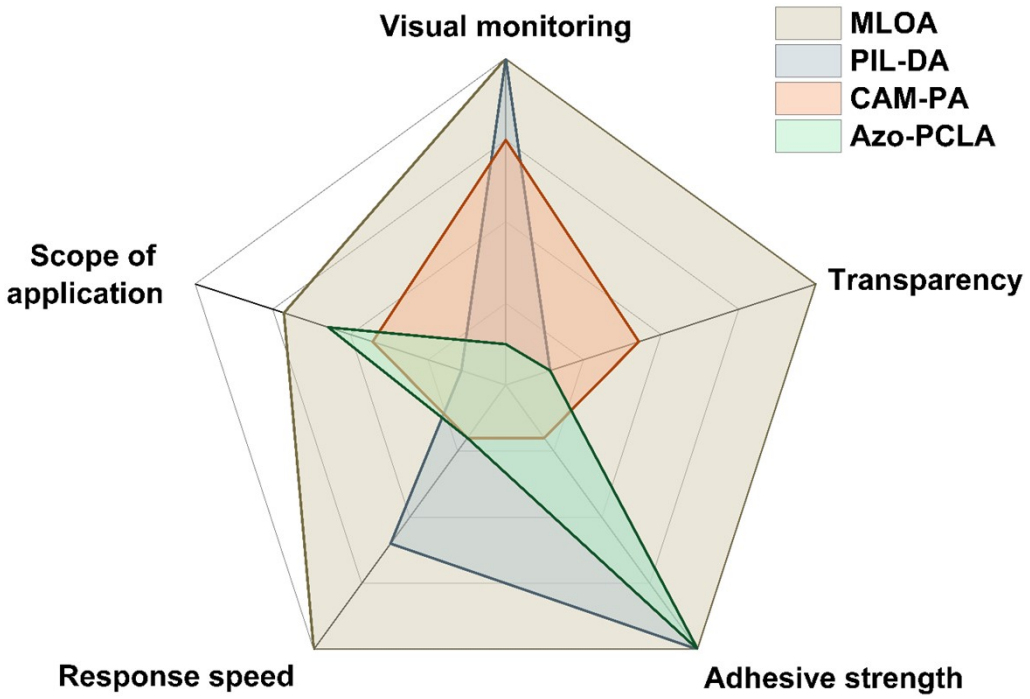

Figure S15. Comparison of MLOA with recently-reported intelligent, real-time, and visual monitoring adhesive in terms of visual monitoring, scope of application, response speed, adhesive strength and transparency.

As shown, MLOA exhibits a balanced and superior profile across all dimensions. Notably, it demonstrates exceptional performance in visual monitoring, transparency, and adhesive strength, outperforming the other systems. This is attributed to its spiropyran-based colorimetric feedback mechanism, biomass-based transparent matrix, and strong oxidative crosslinking of linseed oil. In contrast, the poly(ionic liquid)-detectable adhesives (PIL-DA)system excels in response speed due to its rapid electrical signal response but suffers from poor compatibility with non-conductive substrates and lower transparency. [2] The chameleon adhesive materials-photonic adhesives (CAM-PA) adhesive shows moderate performance across all parameters but lacks distinct advantages. [3] Meanwhile, Azobenzene- polycaprolactone adhesives

(Azo-PCLA) achieves high adhesive strength but is limited by its low transparency and weak visual feedback capability due to the requirement of targeted light activation and restricted molecular mobility. [4] Overall, MLOA's comprehensive advantages in intelligent responsiveness, mechanical performance, and real-time visualization make it a promising candidate for advanced applications in transparent, embedded, or inaccessible bonding environments where traditional testing methods are ineffective.

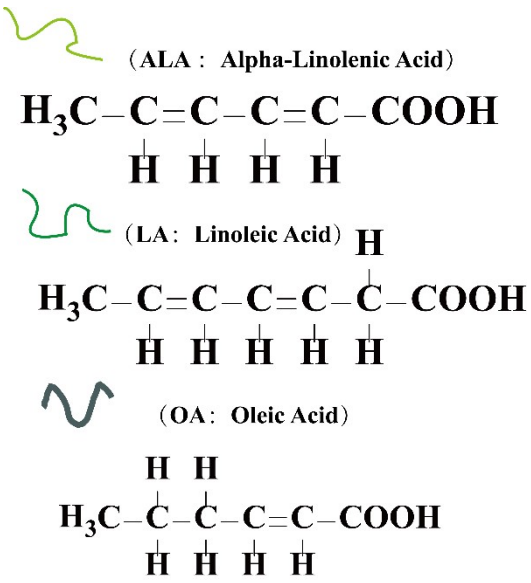

Figure S16. The long chains bend freely, and the linseed oil presents a flowing liquid state.

Linseed oil is one of the most widely used vegetable oil in paints formulation consists of three carbon backnones with long chain unsaturation fatty acids. [5] The long-chain unsaturated fatty acids in linseed oil exhibit a kinked structure from cis-double bonds, creating steric hindrance and larger intermolecular spacing. This reduces van der Waals forces and weakens molecular cohesion, preventing crystallization and maintaining a liquid state with high fluidity at ambient temperatures.

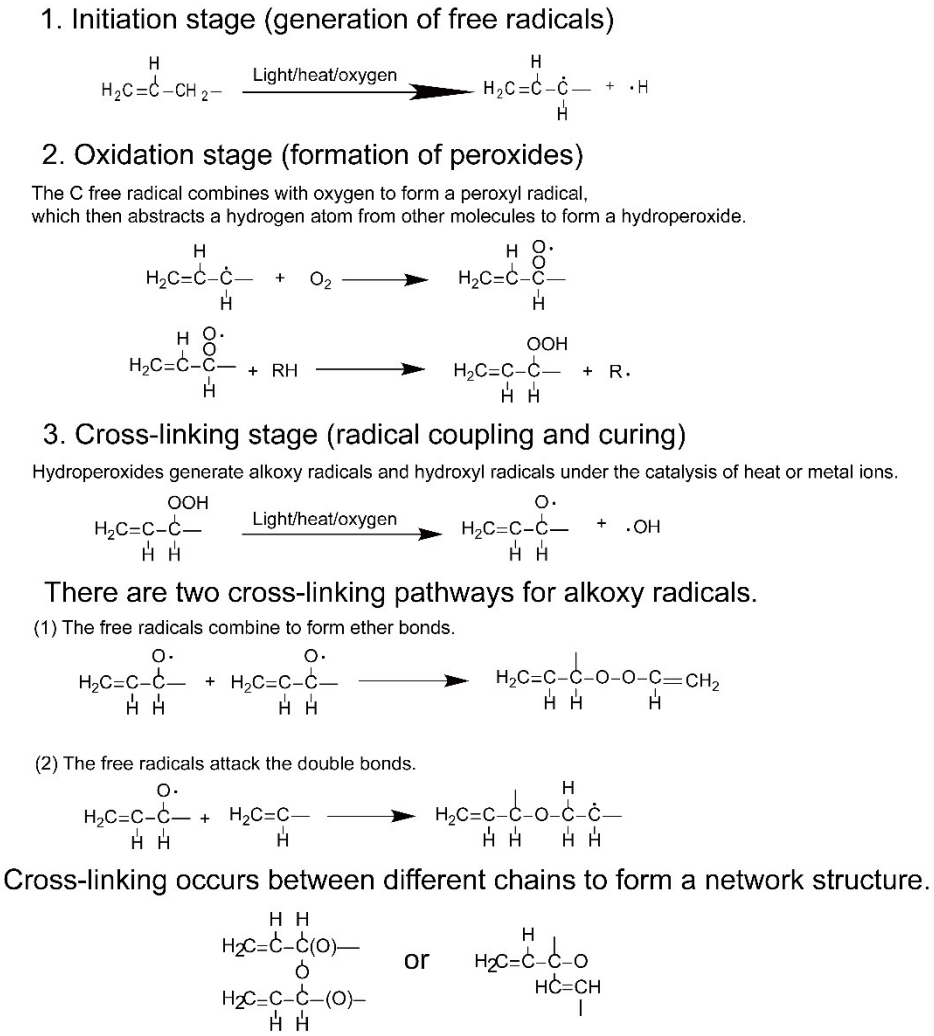

Figure S17. The free radical reaction of linseed oil.

The free radical polymerization of linseed oil is an oxidative cross-linking process involving oxygen. [6] Upon exposure to air, hydrogen atoms are abstracted from the allylic positions of the polyunsaturated fatty acid chains, forming carbon-centered radicals (initiation stage). These radicals rapidly react with molecular oxygen to generate peroxy radicals and hydroperoxides (-OOH) (oxidation stage). Under heat or in the presence of metal ions, the hydroperoxides decompose into alkoxy (-O•) and hydroxyl (•OH) radicals, initiating further radical coupling and crosslinking reactions (curing stage). The alkoxy radicals can either combine directly to form ether linkages

(C–O–C) or add across C=C bonds to create C–C crosslinks, resulting in the formation of a three-dimensional polymeric network. Through these oxidative radical reactions, linseed oil gradually transforms from a liquid triglyceride into a solid crosslinked film.

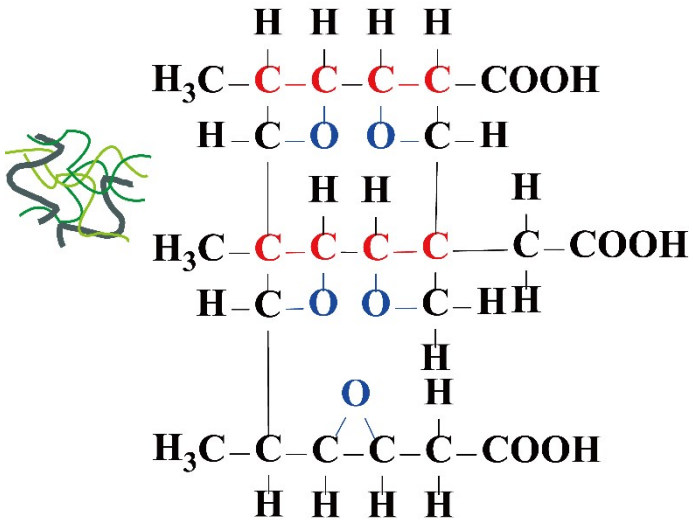

Figure S18. It is fixed by covalent bonds and cannot flow freely, so linseed oil presents a solid state.

Upon exposure to oxygen, the unsaturated fatty acid chains in linseed oil undergo free-radical initiated reactions, leading to the formation of new covalent bonds, such as C-C bonds between different fatty acid chains. As a result, these chains become covalently anchored within a three-dimensional network, which significantly restricts their molecular mobility and leads to the loss of fluidity, thereby contributing to the solidification of the oil.

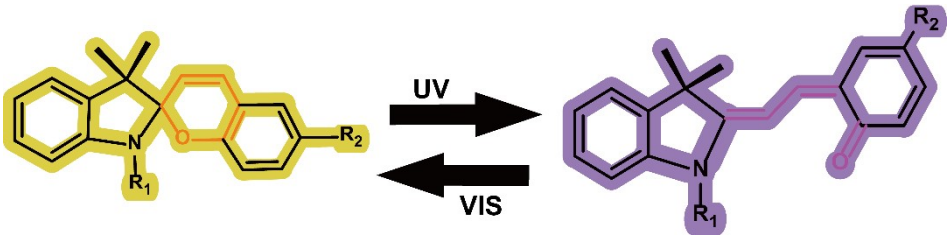

Figure S19. Photochromic mechanism of spiropyran.

Spiropyran (SP), [7] typically containing a benzopyran (chromene) covalently connected to a heterocyclic moiety via the spiro-carbon. The ring-closed structure of SP is typically the thermodynamically stable isomer, which can reversibly transform to the ring-opened form upon exposure to light, the stimuli-responsive SP transformation is accompanied by a vivid color change (i.e., colorless to colored or vice versa).

References

[1] Li, D.; Qing, L.; Li, M.; Cheng, H.; Yang, G.; Fu, Q.; Sun, Y. *Prog. Org. Coat.* **2022**, *166*. DOI: 10.1016/j.porgcoat.2022.106776.

[2] Liu, Z.; Wang, Y.; Wu, M.; Yin, S.; Li, Q.; Cao, Q.; Zheng, S.; Li, W.; Wang, X.; Yan, F. *Adv. Funct. Mater.* **2024**, *35* (3). DOI: 10.1002/adfm.202413799.

[3] Kim, M.; Lee, H.; Krecker, M. C.; Bukharina, D.; Nepal, D.; Bunning, T. J.; Tsukruk, V. V. *Adv. Mater.* **2021**, *33* (42), e2103674. DOI: 10.1002/adma.202103674.

[4] Lin, Z.; Feng, J.; Fang, L.; Zhang, Y.; Ran, Q.; Zhu, Q.; Yu, D. *Adv. Mater.* **2024**, *36* (39), e2406459. DOI: 10.1002/adma.202406459.

[5] Dixit, S.; kanakraj, S.; Rehman, A. *Renewable Sustainable Energy Rev.* **2012**, *16* (7), 4415-4421. DOI: 10.1016/j.rser.2012.04.042.

[6] Turco, R.; Tesser, R.; Russo, V.; Cogliano, T.; Di Serio, M.; Santacesaria, E. *Industrial & Engineering Chemistry Research* **2021**, *60* (46), 16607-16618. DOI: 10.1021/acs.iecr.1c02212.

[7] Kortekaas, L.; Browne, W. R. *Chem. Soc. Rev.* **2019**, *48* (12), 3406-3424. DOI: 10.1039/c9cs00203k.